Journal of Nuclear Materials 384 (2009) 236–244

Contents lists available at ScienceDirect

Journal of Nuclear Materials

journal homepage: www.elsevier.com/locate/jnucmat

Thermal and structural properties of low-fluence irradiated graphite

Dusan Lexa [a,*,1], Michael Dauke [b,2]

[a] Canberra Packard Central Europe GmbH, Wienersiedlung 6, A-2432 Schwadorf, Austria
[b] AGES GmbH, 1226 Vienna, Austria

ARTICLE INFO

Article history:
Received 4 March 2008
Accepted 18 November 2008

PACS:
81.05.T
61.80
81.70.P
61.60

ABSTRACT

The release of Wigner energy from graphite irradiated by fast neutrons at a TRIGA Mark II research reactor has been studied by differential scanning calorimetry and simultaneous differential scanning calorimetry / synchrotron powder X-ray diffraction between 25 and 725 °C at a heating rate of 10 °C min^{-1}. The graphite, having been subject to a fast-neutron fluence from 5.67×10^{20} to 1.13×10^{22} n m^{-2} at a fast-neutron flux ($E > 0.1$ MeV) of 7.88×10^{16} n m^{-2} s^{-1} and at temperatures not exceeding 100 °C, exhibits Wigner energies ranging from 1.2 to 21.8 J g^{-1} and a Wigner energy accumulation rate of 1.9×10^{-21} J g^{-1} n^{-1} m^2. The differential–scanning–calorimeter curves exhibit, in addition to the well known peak at ~200 °C, a pronounced fine structure consisting of additional peaks at ~150, ~230, and ~280 °C. These peaks correspond to activation energies of 1.31, 1.47, 1.57, and 1.72 eV, respectively. Crystal structure of the samples is intact. The dependence of the *c* lattice parameter on temperature between 25 and 725 °C as determined by Rietveld refinement leads to the expected microscopic thermal expansion coefficient along the *c* axis of $\sim 26 \times 10^{-6}$ °C^{-1}. At 200 °C, coinciding with the maximum in the differential–scanning–calorimeter curves, no measurable changes in the rate of thermal expansion have been detected – unlike its decrease previously seen in more highly irradiated graphite.

1. Introduction

Displacement of atoms from their normal lattice positions in solids by fast particles was first predicted by Wigner [1,2]. The resulting entrapment of these atoms at non-lattice points is accompanied by a number of changes in physical characteristics of the solid, including an increase in internal energy, also called Wigner energy. These effects have most frequently been observed and studied in graphite irradiated by fast neutrons, and are especially pronounced following graphite irradiation at low temperatures, i.e., below 100 °C, where no significant *in situ* annealing takes place. Upon heating, the bulk of the stored energy is typically released at and above 200 °C. Its amount can be roughly determined by heating a sample big enough to accept a thermocouple in a laboratory furnace to well above that temperature, e.g., 500 °C, in two separate runs, calculating the temperature difference between the runs, and using the known heat capacity of the sample in the requisite calculation. More sophisticated methods, applicable to samples in the mg range, include differential thermal analysis (a somewhat more accurate variation of the above technique), bomb calorimetry (most accurate in theory but cumbersome in implementation, measures total stored energy directly), and differential scanning calorimetry (DSC) which is the method of choice due to its high accuracy and wide availability of commercial instrumentation. In DSC, the heat flux out of the sample is measured as it is being heated to a maximum temperature usually determined by instrument limitations (725 °C in this study). The stored energy is simply obtained by integration. In cases where the energy release has not ceased upon reaching the maximum temperature, an underestimation of the total Wigner energy will result. While there are in fact indications of Wigner energy release at higher temperatures (1000–1500 °C), e.g., see Rappeneau et al. (Ref. in [12]), this phenomenon seems to be limited to very-highly irradiated specimens and is not expected to play any role in the present work (see Section 2).

In a previous paper [3], the thermal, structural, and radiological properties of irradiated graphite from the ASTRA research reactor have been studied, with a focus on implications for disposal. The study was limited to the graphite from the inner thermal column of the reactor, which became available as a result of the reactor's decommissioning. The main uncertainty was the estimated fast-neutron fluence of between 10^{21} and 10^{24} n m^{-2} to which the graphite should have been exposed over the life time of the reactor.

To verify our results pertaining to the Wigner energy accumulation and the structural changes as a function of fast-neutron fluence, this study has been initiated. DSC and simultaneous DSC / X-ray diffraction (DSC/XRD) have been employed again. The main improvement compared to [3] has been the irradiation of graphite

* Corresponding author.
E-mail address: dusan.lexa@canberra.com (D. Lexa).
[1] Formerly Department of Radioactive Waste Management, Nuclear Engineering Seibersdorf GmbH, 2444 Seibersdorf, Austria.
[2] Formerly Atomic Institute of the Austrian Universities, 1020 Vienna, Austria.

0022-3115/$ - see front matter © 2008 Elsevier B.V. All rights reserved.
doi:10.1016/j.jnucmat.2008.11.013

samples in a controlled fashion resulting in significantly more accurate fast-neutron fluence data. Additionally, the range of fluences has been extended to lower values to explore the fundamentally more interesting 'linear response region' – a range of fast-neutron fluences from zero up to a certain limiting value, where the accumulated Wigner energy is directly proportional to the fluence. Last but not least, a larger number of samples have been measured, and the temperature resolution of the DSC/XRD measurements has been dramatically improved by the use of a novel detector. The inclusion of a more extensive literature review was deemed necessary by the authors attempting a thorough comparison with data accumulated on the subject over more than 60 years since Wigner's original conjecture.

Table 1
Graphite specifications[a].

Types	Artificial graphite baked at not less than 4500 °F
Thermal neutron cross section	4.8 millibarns/atom
Average diffusion length	Not less than 48 cm
Total ash content	700 ppm
Boron	0.8 max. ppm
Porosity	24–25%
Specific resistance (ohm in)	Longitudinal: 0.00030/transverse: 0.00040
Tensile strength (psi)	1400
Flexural strength (psi)	2100
Compressive strength (psi)	6000
Modulus of elasticity $\times 10^6$ (psi)	Longitudinal: 1.5/transverse: 1.1
Thermal conductivity (Btu/h/ft^2/F/ft)	Longitudinal: 90–100/transverse: 65–75
Coefficient of thermal expansion $\times 10^{-7}$ per F	Longitudinal: 8/transverse: 15
Apparent density (g/cm^3)	1.68–1.70

[a] The graphite has originally been manufactured by the American Machine and Foundry Company in 1958. These specifications are a verbatim transcription, including the original units, of a data sheet provided by the manufacturer at that time.

2. Experimental

Twenty five samples were machined from a block of 'unirradiated' graphite originally used in the outermost section of the outer thermal column of the ASTRA research reactor [3]. The graphite specifications are summarized in Table 1. The maximum possible pre-irradiation fluence is estimated at $\sim 10^9$ n m^{-2} (fluence correction applied, see Section 4.1). The disks were 8.0 mm in diameter and 1.0 mm thick, weighing ~80 mg. Machining of the samples on a lathe was done at reduced rpm with alcohol cooling so that the temperature is not expected to have exceeded 25 °C. (However, this precaution designed to prevent Wigner energy release during machining of irradiated graphite samples has no importance here.)

Prior to irradiation, samples were dried in an oven at about 110 °C for one day to release any adsorbed atmospheric moisture. Up to four samples were then sealed in quartz ampoules which were placed in aluminum holders and irradiated. The temperature of the reactor water at a power of 250 kW was about 90 °C. After irradiation, the aluminum holders were removed from the irradiation position but left in the tank for 2 days to allow for the decay of short-lived activation products. The temperature of the reactor water during this decay period was about 34 °C. The samples were then removed and stored in plastic vials until measurement by DSC or DSC/XRD. (In our previous work [3], thermal effects associated with the desorption of moisture from the samples between 25 and 100 °C have not been observed. Some of the current results lead us to believe that this effect might interfere with accurate Wigner energy determination in low-fluence irradiated samples, where the exothermic Wigner energy magnitude becomes comparable with the endothermic water desorption enthalpy. The sample mass loss during the measurements (see Table 2) was ~0.1 mg for all the samples measured within days after irradiation but ~1.0 mg for samples stored for 6 months. Ascribing the entire mass loss to water desorption and using a water-on-active-coal adsorption enthalpy of ~40 kJ mol^{-1} at 25 °C, would lead to an endothermic contribution of between ~3 and ~30 J g^{-1} for an 80 mg sample. There might be several ways to minimize this effect in the future, such as

Table 2
Sample characteristics, measured and derived quantities.

Sample	t (h)	Φ_f (n m^{-2})	m (g)	Δm (mg)	dpa (Eq. (1))	ΔH_{Wigner} (J g^{-1})	ΔH_{Wigner}(J g^{-1})	dpa (Eq. (2))	c at 25 °C (nm)
ATI-1x18-001[a]	40	1.13×10^{22}	0.08469	0.13	1.3×10^{-3}	−24.09	−21.8 ± 1.4	1.9×10^{-4}	–
ATI-1x18-002[a]			0.08392	0.12		−22.22			–
ATI-1x18-003[a]			0.08457	0.05		−21.82			–
ATI-1x18-004[a]			0.08385	0.17		(−26.72)			–
ATI-1x18-005[b]			0.08180	–		−21.28			0.675
ATI-1x18-006[b]			0.08337	–		−19.72			0.675
ATI-5x17-007[a]	20	5.67×10^{21}	0.08339	0.09	6.5×10^{-4}	−9.40	−10 ± 0.5	8.9×10^{-5}	–
ATI-5x17-008[a]			0.08456	0.08		−10.72			–
ATI-5x17-009[a]			0.08437	0.08		−9.69			–
ATI-5x17-010[b]			0.08380	–		−10.24			0.675
ATI-5x17-011[b]			0.08425	–		(−1.31)			0.675
ATI-1x17-018[a]	4	1.13×10^{21}	0.08474	0.12	1.3×10^{-4}	−2.05	−2.2 ± 0.3	2.0×10^{-5}	–
ATI-1x17-019[a]			0.08422	0.13		−2.04			–
ATI-1x17-020[a]			0.08401	0.02		−2.80			–
ATI-1x17-021[c]			0.08396	0.80		−2.21			–
ATI-1x17-022[b]			0.08442	–		(−0.99)			0.675
ATI-1x17-023[b]			0.08493	–		(−0.59)			0.675
ATI-1x17-024[c]			0.08421	1.00		−1.97			–
ATI-1x17-025[c]			0.08464	0.90		(−0.30)			–
ATI-5x16-012[a]	2	5.67×10^{20}	0.08696	0.11	6.5×10^{-5}	−1.52	−1.2 ± 0.4	1.1×10^{-5}	–
ATI-5x16-013[a]			0.08468	0.07		(−4,55)			–
ATI-5x16-014[a]			0.08455	0.07		−1.42			–
ATI-5x16-015[c]			0.08444	0.60		−0.65			–
ATI-5x16-016[b]			0.08347	–		−1.26			(0.675)
ATI-5x16-017[b]			0.08432	–		(−2.71)			0.675

[a] DSC, Pyris Diamond.
[b] DSC/XRD.
[c] DSC, DSC-7.

storage of the samples in a desiccator, opening the (evacuated) quartz ampoules just prior to measurement, preceding the actual measurement with an extended period of high-purity Ar purge in situ, etc.)

Samples have been irradiated at the TRIGA Mark II research reactor of the Atomic Institute of the Austrian Universities in Vienna [4]. The irradiation of the samples was performed in the Central Irradiation Channel (CIC), which is situated in the centre of the reactor core. In the CIC, which can accommodate samples with diameters up to 38.4 mm, both neutron flux and the fraction of high energy neutrons exhibit a maximum in the horizontal plane. The vertical position of the neutron flux maximum within the CIC is 340 mm below the top of the reactor grid. The total flux at the CIC as well as the flux of thermal and fast neutrons is 2.1×10^{17}, 6.1×10^{16} ($E < 0.55$ eV), 7.6×10^{16} ($E > 0.1$ MeV), and 4.0×10^{16} ($E > 1$ MeV) n m^{-2} s^{-1}, respectively [4]. The fast ($E > 0.1$ MeV) neutron flux measured at 15 kW and extrapolated to 250 kW for this series of experiments is 7.88×10^{16} n m^{-2} s^{-1}. Multiplication with the irradiation time of 2, 4, 20, and 40 h, respectively, yields the fast-neutron fluence (see Table 2).

DSC experiments were performed with power-compensated instruments PerkinElmer DSC-7 and PerkinElmer Pyris Diamond. The DSC-7 settings were: ice-water cooling (0 °C), 99.9999% Ar purge gas at 20 cm^3 min^{-1}, temperature range 25–625 °C, heating rate 10 °C min^{-1}. The Pyris Diamond settings were: circulating-liquid chiller cooling (−5 °C), 99.9999% Ar purge gas at 20 cm^3 min^{-1}, temperature range 25–725 °C, heating rate 10 °C min^{-1}.

DSC/XRD experiments were performed on the Materials Science insertion device beam line at the Swiss Light Source at Paul Scherrer Institute [5] with an instrument described previously [6]. It essentially consists of a PerkinElmer DSC sample holder modified to allow for simultaneous XRD, attached to a diffractometer, and a remotely connected PerkinElmer Pyris 1 DSC instrument. The Pyris 1 DSC settings were: circulating-liquid chiller cooling (−10 °C), 99.9999% Ar purge gas at 20 cm^3 min^{-1}, temperature range 25–725 °C, heating rate 10 °C min^{-1}. Compared to previous experiments [3] involving 2θ scanning, a novel position-sensitive X-ray microstrip detector [7] has been employed. Because of a short readout time, the temperature resolution has been improved dramatically, with each DSC scan accompanied by a full 2θ XRD snapshot approximately every 2 °C. A cryogenically cooled Si(1 1 1) double-crystal monochromator was used to select the incident beam wavelength of 0.0925 nm (13.4 keV). The intrinsic resolution of the curved detector positioned at a distance of 76 cm from the sample is 0.004° with a 2θ angular coverage of 60°. The angular positioning of the detector was such that the effective 2θ range was 0–55° which was further reduced for data analysis to 5–50°. XRD patterns were evaluated by Rietveld refinement (a standard mathematical procedure for extracting the maximum of structural information from powder XRD patterns) using the GSAS software package [8] with only background, profile coefficients, histogram scale factors, diffractometer zero, and lattice parameters c and a being optimized.

In both DSC and DSC/XRD experiments, two identical scans were performed with each sample. The heat flux measured by DSC in the first run is a result of the sample heat capacity and the release of the Wigner energy, while in the second run only heat capacity should contribute to the heat flux, assuming complete Wigner energy release in the first run [3]. Hence, subtraction of the second-run from the first-run data (including, in some cases, a linear correction for baseline drift), division by sample mass, and integration over a specified temperature range, yields the specific Wigner energy released in the first run. Even though the experiments have been carried out between 25 and 725 °C (625 °C), the integration only extended between 25 and 375 °C due to signal instability at higher temperatures. However, the Wigner energy release above 375 at 10 °C min^{-1} should be insignificant as was the case with even more highly irradiated samples [3]. The small endothermic features observed in some samples between 25 and 100 °C and thought to be associated with water desorption have also been corrected for.

3. Theory and calculations

3.1. Graphite irradiation by fast neutrons and Wigner energy release

Displacement of atoms from their normal lattice positions in solids by fast particles was first predicted by Wigner in 1942 [1,2, in 9]. Assuming that the fraction of the neutron energy transferred into translational energy of the carbon atom was unity, he showed that fast neutrons produced in the fission of uranium would possess enough energy to displace $\sim 2 \times 10^4$ carbon atoms per neutron. Teller [in 9] estimated that only about half of the kinetic energy of a 2 MeV neutron is lost by elastic collisions with carbon atoms and that the remainder is dissipated harmlessly by electronic excitation and ionization, proportionately reducing the number of displaced carbon atoms per neutron. Subsequent calculations by Seitz [10] put the number closer to $\sim 2 \times 10^3$, assuming carbon primary knock-on atoms to be effective in elastic collisions with other carbon atoms only below a certain critical energy and a carbon atom displacement energy of ~25 eV. (A 2 MeV neutron has to undergo 21.1 collisions with carbon atoms loosing 0.158 of its energy in each collision and reducing its energy to ~53 keV before the energy of the primary knock-on atoms falls below the critical energy of 8.4 keV). In [9], citing [10], the critical energy of the primary knock-on atoms is given as 11 keV (possibly because a rough value of 1/7 = 0.14 has been used for the energy loss factor of the neutron) and the number of displaced carbon atoms per primary knock-on atom as 90. This would also result in the value for the critical neutron energy of ~83 keV and the displacement of $\sim 3 \times 10^3$ carbon atoms per neutron. Also in [9], a carbon atom displacement energy of 13 eV, derived from the heat of sublimation of graphite, is mentioned. This would increase the number of displaced carbon atoms per neutron by a factor of 2.) Finally in [9], more recent theoretical calculations are referenced, increasing the number of displaced carbon atoms per neutron and per primary knock-on atom from 2000 to 6000 and from 90 to 180, respectively. Thrower and Mayer [11] quote yet another value of 500 displacements per 1 MeV neutron. Values of interaction parameters of fast neutrons in graphite are summarized in Table 3.

The resulting entrapment of the displaced atoms at non-lattice points and the creation of vacancies are accompanied by a number of changes in physical characteristics of the solid, such as a decrease in thermal conductivity and a lattice parameter, and an increase in elastic modulus, electrical resistance, breaking strength, c lattice parameter and internal (Wigner) energy [9]. Upon heating to sufficiently high temperatures, the displaced atoms presumably diffuse back to the vacancies. The energy, released as heat, can be measured by standard calorimetry techniques. There is still mostly speculation about the nature of the Wigner energy buildup and release at the atomic level. The number of displaced atoms and vacancies is, on a macroscopic level, determined by the fast-neutron fluence and the displacement cross section. The associated Wigner energy depends on (the distribution of) the magnitudes of the individual defect energies. Each of these variables is discussed below.

3.2. Fast-neutron fluence

Our previous work [3] was an examination of graphite removed from the thermal column of a research reactor decommissioned

Table 3
Selected parameters for the displacement of carbon atoms in graphite by fast neutrons (E = 2 MeV).

	σ_d (m^2)	dpn	E_i (keV)	ϵ_i (eV)	E_d (eV)	h_F (eV)
Wigner [1,2,9], p. 4		20000	2000		100?	
Teller [9], p. 126		10000?	1000		100?	
Seitz [10]		2000	53	8390	25	
Neubert [9], p. 62, 63	3.6×10^{-26}	2000 (6000)	83	11000	25 (13)	
Primak [14]	10^{-25}					14
Iwata et al. [15]	11.5×10^{-26}					
Mitchell and Taylor [17]					60	13.5
Bochirol and Bonjour [18]					35	9.5
Bonjour et al. [13]					35	8.5
Thrower and Mayer [11]	?	500[a]			40	14
Iwata [16]						18
Kelly et al. [12]					25–60	
Telling et al. [20]						13–15 (10.6)[b]
Ewels et al. [21]						13.7 (10.8)[b]

[a] 1 MeV neutron.
[b] Intimate Frenkel pair.

after 39 years of service – an autopsy of sorts. The fast-neutron fluence ascribed to every graphite sample was a value arrived at by estimating the fluence at a position closest to the reactor core and taking into account the attenuation caused by the neutrons passing through varying thicknesses of graphite to the sample positions. As the attenuation effects in graphite are well known, the accuracy hinged solely on the estimated fast-neutron fluence of 1.7×10^{24} n m^{-2} at the entrance to the thermal column. Because of the uncertainties involved, the value might deviate from the true one by as much as an order of magnitude. This unsatisfactory situation has been addressed in this work by irradiating graphite samples in a controlled fashion. The relative accuracy of current fast-neutron flux and, hence, fluence values is ±11.6% [4].

The range of fast-neutron fluences covered in this work has been chosen to extend to lower values (with still measurable Wigner energy release) and to overlap with the low end of the previous fluence range in order to explore in more detail the properties and the extent of the 'linear response region' as well as to offer a consistency check with the previous data. As already mentioned in the introduction, under 'linear response region' we understand a range of fast-neutron fluences from zero up to a certain limiting value, where the accumulated Wigner energy is directly proportional to the fluence. This implies that the displacements per atom (dpa) are sufficiently low so that Frenkel defects do not interact with each other and the individual Frenkel defect energy, h_F, (see below) is constant. Our previous work (fluence correction applied, see Section 4.1) suggests that these conditions are met below 6×10^{22} n m^{-2}, i.e., dpa $\approx 8 \times 10^{-3}$. Henson and Reynolds (Ref. in [12]) found that h_F decreases substantially for dpa > 0.1 while Bonjour et al. [13] concluded that there was decrease in the accumulated Wigner energy per unit fluence at fluences greater than 10^{22} n m^{-2} (E > 1 MeV), i.e., dpa $\approx 1 \times 10^{-3}$.

The comparison with other literature data is somewhat complicated by two problems. The first is the indiscriminate use of the terms 'fast' neutrons, 'fast-neutron' fluence, etc. In this work, these refer to neutron energies greater than 0.1 MeV. Other meanings, e.g., E > 1 MeV, are explicitly noted. The importance of careful source characterization for a comparison of irradiation damage studies has been pointed out previously [4]. In the case of the TRIGA Mark II reactor for instance, $\varphi(E > 0.1\ \text{MeV}) = 1.9\varphi(E > 1\ \text{MeV})$ [4], which might not be the case at other irradiation facilities. The interesting question of relative contributions of different parts of the fast-neutron spectrum to the radiation damage and Wigner energy accumulation, i.e., the establishment of $\sigma_d(E = 0.1 - 1\ \text{MeV})$ and $\sigma_d(E > 1\ \text{MeV})$ or, better yet, differential displacement cross sections $\sigma_d(E, E + dE)$ for E > 0.1 MeV, has to the best of our knowledge not been attempted yet. The second issue is the fact that identical graphite samples irradiated to the same fast-neutron fluence but exposed to different flux and, hence, irradiated for a different amount of time will, in general, exhibit nonidentical property changes. What is known is that the sample irradiated quickly will show the larger changes [12,14]. For instance, the radiation damage and Wigner energy accumulation in the ASTRA graphite irradiated over the course of 39 years would have to be no higher than that seen in the graphite irradiated at the TRIGA Mark II reactor for a maximum of 40 h.

3.3. Displacement cross section

The connection between the fast-neutron fluence, Φ_f, and the number of atoms displaced, i.e., the number of Frenkel defects formed in the absence of recombination and/or annealing, is provided by the displacement cross section, σ_d

$$n_F = \sigma_d \cdot \Phi_f, \tag{1}$$

with n_F equivalent to the displacements per atom (dpa) if dpa < 1. σ_d can be considered the product of the primary scattering cross section, σ_p, and the number of atoms displaced by a single primary fast carbon recoil, dpp. Taking these quantities to be 4×10^{-28} m^2 and 90, respectively, Neubert et al. [9] arrived at $\sigma_d = 3.6 \times 10^{-26}$ m^2. Although the values of the scattering cross section and the number of displacements per carbon recoil were later shown to be about a factor of three too high and too low, respectively, fortuitous cancellation of errors left σ_d unchanged [9]. From a careful analysis of results from several sources, Primak [14] obtained $\sigma_d = 10^{-25}$ m^2 within a factor of two. The results of more recent studies of displacement cross section of graphite (and other materials) have been summarized by Iwata et al. [15]. The experimental value for graphite therein, used throughout this paper and also in [16], is 11.5×10^{-26} m^2. Other theoretical values from [15] include 11.2×10^{-26} m^2 and 7.4×10^{-26} m^2. The graphite cross section data are summarized in Table 3. Hence, n_F can be calculated for any graphite sample using the value of Φ_f the sample has been exposed to. With an accurately known Φ_f, the accuracy of n_F depends solely on that of σ_d.

3.4. Frenkel defect energy

The recombination of interstitials and vacancies, also known as Frenkel pairs, is considered to be the key step in Wigner energy release. Mitchell and Taylor [17] studied electron-irradiated graphite and concluded that for an atomic displacement energy of E_d = 60 eV the Frenkel pair energy is 13.5 eV. The subambient irradiation work of Bochirol and Bonjour [18] and Bonjour [13] yielded Frenkel pair formation energies of 9.5 and 8.5 eV, respectively. The determinations of Frenkel pair energy from Wigner energy measurements [13,17–19] have been reviewed by Thrower and Mayer [11]. The result, 14 ± 1 eV for a displacement energy E_d = 40 eV, is somewhat difficult to justify considering the experimental values [13,17–19]. Iwata [16] estimated the energy released in an annihilation of a Frenkel pair to be 18 eV. In their quantum-mechanical study, Telling et al. [20] concluded that a number of defect species form strong covalent bonds between the graphite atomic layers, calculated the energy released in a Frenkel pair recombination as 13–15 eV per pair, and also intro-

duced a close-bound or intimate Frenkel pair with an energy of formation of 10.6 eV and a barrier to recombination of 1.4 eV. In another quantum-mechanical study, Ewels et al. [21] examined the structures and recombination routes for Frenkel pairs in irradiated graphite. The energy of formation of a widely separated Frenkel pair is calculated as 13.7 eV, while that of the intimate Frenkel pair is given as 10.8 eV with and a barrier to recombination of 1.3 eV. The recombination of the intimate Frenkel pair is suggested as the cause of the Wigner energy release peak observed around 200 °C. Selected values of atomic activation energy and Frenkel pair energy are summarized in Table 3. In the linear response region, a simple relationship between the specific Wigner energy, ΔH_{Wigner}, Frenkel defect energy, h_{F}, and n_{F} can be established:

$$n_{\text{F}} = \frac{M_{\text{C}} \cdot \Delta H_{\text{Wigner}}}{N_{\text{A}} \cdot h_{\text{F}}} = \frac{\rho_{\text{C}} \cdot \Delta H_{\text{Wigner}}}{\upsilon_{\text{C}} \cdot h_{\text{F}}}, \tag{2}$$

where N_{A} is Avogadro's number, and M_{C} is the molar mass, υ_{C} the density, and υ_{C} the number of atoms per unit volume of graphite. This equation enables the dpa calculation from the experimentally determined ΔH_{Wigner} and the theoretical value of h_{F}. Ideally, the dpa values obtained from Eqs. (1) to (2) should be identical. Any discrepancies would point to inaccuracies in one or more of the values of ΔH_{Wigner} (directly measured), Φ_{f} (indirectly measured), σ_{d} (indirectly measured), and h_{F} (theoretical) or to the breakdown of this simple model beyond the linear response region. In other words, the ratio of n_{F} obtained from Eqs. (1) and (2) should be unity

$$\frac{\sigma_{\text{d}} \cdot \Phi_{\text{f}} \cdot N_{\text{A}} \cdot h_{\text{F}}}{M_{\text{C}} \cdot \Delta H_{\text{Wigner}}} = \frac{\upsilon_{\text{C}} \cdot \sigma_{\text{d}} \cdot \Phi_{\text{f}} \cdot h_{\text{F}}}{\rho_{\text{C}} \cdot \Delta H_{\text{Wigner}}} = 1. \tag{3}$$

3.5. Wigner energy

The magnitude of the Wigner energy in graphite has first been accurately measured using a simple DTA apparatus [9]. Samples irradiated at the Oak Ridge graphite pile for 54 MW-days at <100 °C and 175 MW-days at <130 °C exhibited an energy release of 9 and 29 J g^{-1}, respectively, upon heating from room temperature to 300 °C at 2 °C min^{-1}. Heating to 500 °C increased these values by an estimated 10%. The neutron-irradiated graphite samples in the study of Mitchell and Taylor [17] exhibited a Wigner energy release of 90.3 J g^{-1} at a fast-neutron fluence of 2.5×10^{22} n m^{-2}. They also cited the results of Äström for irradiation at 35 °C: 22.26 J g^{-1} at a fast-neutron fluence of 3.8×10^{21} n m^{-2}. When it was realized that significant annealing of the defects accompanied by a reduction of the Wigner energy takes place even at room temperature, a number of studies at cryogenic temperatures were initiated. Bochirol et al. [19] irradiated graphite at −195 °C to a fast-neutron fluence of between 2.0 and 8.2×10^{22} n m^{-2} ($E > 1$ MeV) and measured the Wigner energy release between −173 and 227 °C. Bochirol and Bonjour [18] irradiated graphite with neutrons at −246 and −196 °C. The Wigner energy release between −213 and 327 °C was 68.04 J g^{-1} at a fast-neutron fluence of 4.96×10^{21} n m^{-2} ($E > 1$ MeV). Bonjour et al. [13] irradiated graphite to fast-neutron fluences between 10^{21} and 10^{22} n m^{-2} ($E > 1$ MeV) at −196 °C and measured the Wigner energy release between −196 and 297 °C the magnitude of which followed the formula $301.2[1 - e^{-0.0889\Phi}]$ cal g^{-1}., i.e., $1265[1 - e^{-0.0889\Phi}]$ J g^{-1}. (This is repeated in Kelly [12] as $1259[1 - e^{-0.0889\Phi}]$ J g^{-1}. Throughout this work we have used the approximate relation 1 cal = 4.2 J to convert older data. Using the exact factor of 4.184 in this case would lead to 1260 J g^{-1}. The origin of the 1259 is, therefore, not clear.) However, for the fluences of interest, e.g., 10^{22} n m^{-2}, the exponential term is zero, the bracket is unity, and the Wigner energy is constant at 1265 J g^{-1}. Closer scrutiny of the original data, Fig. 5 in [13], Eq. (8), and the table following Eq. (8), reveals that the correct formula should no doubt involve -0.0889×10^{-18} instead of just −0.0889, yielding, e.g., 107.6 J g^{-1} (25.6 cal g^{-1}) for a fast-neutron fluence of 10^{22} n m^{-2}. Kelly et al. [12] have extensively reviewed irradiation damage in graphite due to fast neutrons, including the accumulation and release of Wigner energy. The Wigner energy content exhibits saturation at high fluences and there is a large effect of irradiation temperature, the rate of energy accumulation decreasing with increasing temperature. Iwata [16] has investigated the magnitude and the kinetics of the Wigner energy release from graphite irradiated to a fluence of 4×10^{21} n m^{-2} at ~80 °C by DTA between room temperature and 350 °C at heating rates from 1 to 100 °C min^{-1}. He obtained a value of 8 ± 1 J g^{-1} and proposed a kinetic model of the Wigner energy release involving three activation energies of 1.34 eV, 1.50 eV, and 1.78 (and three different frequency factors), respectively, arrived at by modeling the DSC curves as a superposition of three Gaussian peaks. However, this method seems to lead to somewhat arbitrary results dependent upon the frequency factor(s) used [22]. Platonov et al. [23] investigated a decommissioned graphite plunger from an RBMK nuclear power reactor exposed to $\sim 0.75 \times 10^{25}$ n m^{-2} ($E > 0.18$ MeV) at 50–80 °C. They estimated the Wigner energy from unreferenced $\Delta H_{\text{Wigner}}(\Phi_{\text{f}}, T)$ correlations at ~840 J g^{-1}.

The comparison between reported data is greatly facilitated by the Wigner energy accumulation per unit of fluence, $\alpha_{\Delta H}$:

$$\Delta H_{\text{Wigner}}(\Phi_{\text{f}}) = \alpha_{\Delta H} \cdot \Phi_{\text{f}}, \tag{4}$$

with $\alpha_{\Delta H}$ expected to be constant in the linear response region. Primak [14] reported a value of $0.2–0.7 \times 10^{-21}$ J g^{-1} n^{-1} m^2. Several other values of $\alpha_{\Delta H}$ are summarized in Table 4. Substituting ΔH_{Wigner} from Eq. (4) into Eq. (3) leads to an expression for the equivalence of dpa calculated from fast-neutron fluence (Eq. (1)) or from the Wigner energy (Eq. (2)), respectively, in the linear response region:

$$\frac{\sigma_{\text{d}} \cdot N_{\text{A}} \cdot h_{\text{F}}}{M_{\text{C}} \cdot \alpha_{\Delta H}} = \frac{\upsilon_{\text{C}} \cdot \sigma_{\text{d}} \cdot h_{\text{F}}}{\rho_{\text{C}} \cdot \alpha_{\Delta H}} = 1. \tag{5}$$

The saturation of ΔH_{Wigner} at higher fluences can be empirically accounted for by a simple rational function [3]:

$$\Delta H_{\text{Wigner}}(\Phi_{\text{f}}) = \frac{a \cdot \Phi_{\text{f}}}{b + \Phi_{\text{f}}}, \tag{6}$$

which is of the same form as the dependence of the fractional increase in electrical resistivity of graphite on fluence observed previously [9].

3.6. Dimensional changes

Irradiation of graphite by fast neutrons can lead to macroscopic dimensional changes, both swelling and shrinkage, of considerable magnitude. The effect, dependent on the type of graphite, fast-neutron fluence, and irradiation temperature, is of prime importance in reactor design. The focus of this work is, however, limited to the fast-neutron irradiation induced changes of the microscopic graphite crystal lattice parameters normally obtained from X-ray diffraction data. (The connection between the macroscopic and microscopic dimensional changes of graphite upon irradiation has, e.g., been reviewed by Kelly et al. [12].) Generally, expansion in the direction perpendicular to the basal planes (c) and contraction in the direction parallel to them (a) has been observed, although the relative magnitudes of the changes depend upon the exposure conditions. X-ray diffraction patterns of highly irradiated graphite exhibit broad and asymmetric peaks suggesting a decrease in the degree of crystallinity [3,12]. Primak [14] reported results by Keating. Graphite irradiated at subambient temperature

Table 4
Wigner energy accumulation and *c* lattice parameter increase rates.

References	$T_{irradiation}$ and $T_{release}$ (°C)	Φ_f (n m^{-2})	$\alpha_{\Delta H}$ (J g^{-1} n^{-1} m^2)	$\alpha_{\Delta c}$ (nm n^{-1} m^2)
Primak [14]	35–60 (−170 to −130)		$0.2\ (0.7) \times 10^{-21}$	$0.34\ (0.60) \times 10^{-25}$
Åström (in [17])		3.8×10^{21}	6×10^{-21}	
Mitchell and Taylor [17]		2.5×10^{22}	4×10^{-21}	
Bochirol [19]	−195/0–227	$2.0–8.2 \times 10^{22}$	4.5×10^{-21}	
Bochirol and Bonjour [18]	−196/27–327	4.96×10^{21}[a]	8.8×10^{-21}	
Bonjour [13]	−196/27–297	$10^{21}–10^{22}$	7.2×10^{-21}	
Iwata [16]		4.0×10^{25}	2×10^{-21}	
Platonov et al. [23]	100 (30)	0.75×10^{25}	$0.12\ (0.14) \times 10^{-21}$	0.4×10^{-26}
Kelly et al. [12]	150 (200)	$1.6\ (2.5) \times 10^{25}$		$0.55\ (0.21) \times 10^{-26}$
Lexa and Kropf [3]	100/25–725	$1.4 \times 10^{22}–1.4 \times 10^{25}$ ($1.8 \times 10^{21}–1.7 \times 10^{24}$)	0.9×10^{-21}[b] (7×10^{-21}[c])	
This work	100/25–375	$5.67 \times 10^{20}–1.13 \times 10^{22}$[d]	$1.9 \pm 0.1 \times 10^{-21}$	0.9×10^{-26}
This work and [3]	100/25–725 (375)	$5.67 \times 10^{20}–1.4 \times 10^{25}$[e]	$0.9 \pm 0.4 \times 10^{-21}$	

[a] ΔH_{Wigner} estimated as 64% of total energy release [13].
[b] Fluence correction applied.
[c] Fluence correction not applied.
[d] From Eq. (4).
[e] From Eq. (6).

exhibited an increase in *c* of 0.006 nm at a fluence of 2×10^{23} n m^{-2}. In analogy to Eq. (4) one can define the increase of *c* per unit fluence, $\alpha_{\Delta c}$:

$$\Delta c(\Phi_f) = \alpha_{\Delta c} \cdot \Phi_f. \quad (7)$$

From the data of Keating, Primak [14] estimates $\alpha_{\Delta c}$ to be 0.60×10^{-25} nm n^{-1} m^2. Irradiation at ambient temperatures lead to a value of 0.34×10^{-25} nm n^{-1} m^2 which was constant up to $>10^{24}$ n m^{-2} and insensitive to the kind of graphite. A much smaller decrease in *a* has also been observed [14]. The review of Kelly et al. [12] encompassed a number of studies under a variety of temperature and fluence conditions. In an irradiation at −196 °C, the changes of $\Delta c/c$ were found to be linear with fluence up to 3×10^{21} n m^{-2} ($\varphi = 1.1 \times 10^{17}$ n m^{-2} s^{-1}, $E > 0.1$ MeV). In another study, the lattice parameter changes seem to be linear with fluence up to 3×10^{22} n m^{-2}. Irradiations between 30 and 1050 °C yielded $\Delta c/c$ values up to 0.15 at the lower temperatures. An experiment at 150 °C yielded a 13% increase in $\Delta c/c$ at a fluence of 1.6×10^{25} n m^{-2} ($\alpha_{\Delta c} = 0.55 \times 10^{-26}$ nm n^{-1} m^2 with $c = 0.67079$ nm [12]) with a continued increase at a reducing rate. At 200 °C, $\Delta c/c$ saturated at 8% at a fluence of 2.5×10^{25} n m^{-2} ($\alpha_{\Delta c} = 0.21 \times 10^{-26}$ nm n^{-1} m^2) accompanied by a change in $\Delta a/a$ of −2%. Platonov et al. [23] determined the *c* and *a* lattice parameters of the RBMK plunger graphite ($\sim 0.75 \times 10^{25}$ n m^{-2}, $E > 0.18$ MeV) from the 002 and 100 X-ray diffraction lines. They obtained $c = 0.704–0.707$ nm and $a = 0.244–0.245$ nm, i.e., $\Delta c/c = 4.22–4.70\%$ and $\Delta a/a = -0.41\%$ to -0.46%. This would yield $\alpha_{\Delta c} = 0.4 \times 10^{-26}$ nm n^{-1} m^2 with $c = 0.675$ nm. Also in [23], a linear correlation between Wigner energy and *c* lattice parameter is presented which, conveniently recast as $\alpha_{\Delta H}/\alpha_{\Delta c}$, amounts to $\sim 3 \times 10^4$ J g^{-1} n m^{-1}.

3.7. Coefficient of thermal expansion

Besides its theoretical value, the coefficient of thermal expansion (CTE) of graphite is also of considerable importance for practical applications. Numerous literature values of the microscopic CTE at ambient temperature cover the range $\alpha_c = 2.31–2.83 \times 10^{-5}$ °C^{-1} and $\alpha_a = -1.0$ to -1.5×10^{-6} °C^{-1}. On the other hand, data on the temperature dependence of the CTE are scantier. Touloukian's results for pyrolytic graphite [24] are (temperatures in °C) $\alpha_c^{20} = 2.31 \times 10^{-5}$ °C^{-1} to $\alpha_c^{1227} = 2.86 \times 10^{-5}$ °C^{-1} and $\alpha_a^{20} = -0.6 \times 10^{-6}$ °C^{-1} to $\alpha_a^{1227} = 2.5 \times 10^{-6}$ °C^{-1}. Khodolenko et al. [25], citing work of Grigoriev and Melikhov gives values ranging from $\alpha_c^{-73} = 2.49 \times 10^{-5}$ °C^{-1} to $\alpha_c^{227} = 2.81 \times 10^{-5}$ °C^{-1} and $\alpha_a^{-73} = -1.33 \times 10^{-6}$ °C^{-1} to $\alpha_a^{127} = -0.91 \times 10^{-6}$ °C^{-1}. Irradiation of graphite by fast neutrons seems to affect the CTE. For instance, the typical values (20–100 °C) of $\alpha_c = 2.6 \times 10^{-5}$ °C^{-1} and $\alpha_a = -1 \times 10^{-6}$ °C^{-1}, have changed to 1.4×10^{-5} °C^{-1} and 1×10^{-6} °C^{-1}, respectively, upon irradiation below 300 °C to above $1–5 \times 10^{24}$ n m^{-2} [12].

4. Results and discussion

4.1. Wigner energy

A set of DSC plots obtained with one set of samples spanning the full fast-neutron fluence range in the course of a DSC experiment is shown in Fig. 1. Between 25 and 375 °C, all samples exhibit exothermic behavior with a maximum rate of heat release around 200 °C. (The small endothermic features between 25 and 100 °C as well as the signal instabilities above 375 °C are discussed in Section 2.) The main 200 °C peak has been observed many times before [3,9,13,16,18,19], and has been ascribed to widely spaced or intimate Frenkel pair recombination [16,20,21]. The additional peaks at higher temperatures – the so called fine structure – are also not new, having been observed previously [3,9,13,16,18,19]. Here, they appear at approximately 230 and 280 °C and agree very well with Iwata's [16] data (peaks B and C) at 10 °C min^{-1}. They are

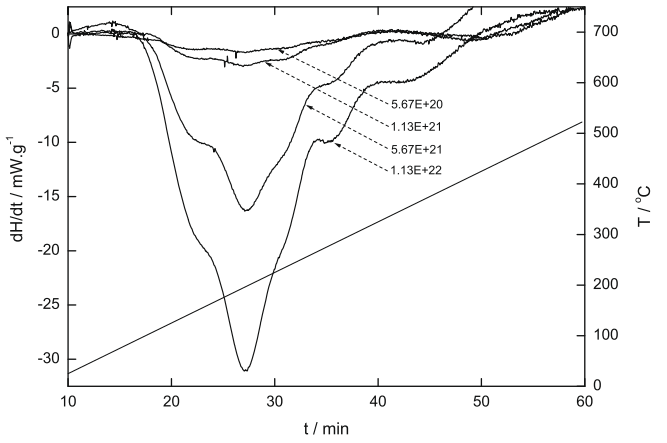

Fig. 1. DSC curves between 25 °C and 525 °C at 10 °C.min^{-1}. Sample mass ~80 mg, heavy line – heat flow, thin line – temperature. Numbers inside the graph represent fluences in n m^{-2}.

apparently a signature of processes with higher activation energy than the Frenkel pair recombination responsible for the 200 °C peak. What seems to be new in the current data is the manifestation of an additional peak at a lower temperature of ~150 °C. It is present in all samples and its relative contribution to the total Wigner energy release seems to increase with decreasing fast-neutron fluence. This peak is found neither in the comparable data of Neubert et al. [9] or Iwata [16] nor in our previous work [3] and indicates a process with an even lower activation energy then the main event at 200 °C. Exothermic peaks below 200 °C have, however, been detected in graphite irradiated at and subsequently heated from cryogenic temperatures [13,18,19]. The absence of the 150 °C peak in previous data could conceivably be the result of higher than assumed irradiation temperature [9], prolonged storage of irradiated material at room temperature prior to measurement [3], attainment of higher temperature upon sample machining [3,9,16], or any combination thereof.

Decomposition of the DSC curves in Fig. 1 into 4 Gaussian peaks [16], without constraining either their FWHM or area, yielded peak temperatures of 150 °C, 200 °C, 230 °C, and 280 °C, respectively. Assuming a frequency factor of 7.5×10^{13} s^{-1} [14,22] and using the equation relating the activation energy, frequency factor, and peak temperature [16,22], activation energies of 1.31 eV, 1.47 eV, 1.57 eV, and 1.72 eV, respectively, have been obtained. This compares with 1.34 eV, 1.50 eV, and 1.78 eV of Iwata, employing variable frequency factors [16], and with 1.47 eV, 1.51 eV, and 1.74 of [12] using 7.5×10^{13} s^{-1}. The agreement is rather good, confirming the notion that while the results so obtained are non-unique [22], i.e., that various combinations of activation energies and frequency factors lead to essentially the same results, the outcome is much more sensitive to the activation energy than to the frequency factor. Also, the fitting sessions showed that while the Gaussian peak positions were more or less constant, FWHMs and peak areas, both related to the frequency factor, varied within wide ranges without discernible changes in the DSC curve. Hence, the relative contribution of different peaks to the total Wigner energy release has not been investigated any further.

The results of the Wigner energy calculation from the DSC plots are given in Table 2 as well as in Fig. 2. Each data point is an average of measurements on four or five samples. The values in parentheses in Table 2 have been discarded as outliers. The Wigner energy ranges from 1.2 J g^{-1} for samples exposed to a fast-neutron fluence of 5.67×10^{20} n m^{-2} to 21.8 J g^{-1} for samples exposed to 1.13×10^{22} n m^{-2}. The dependence of Wigner energy on fluence

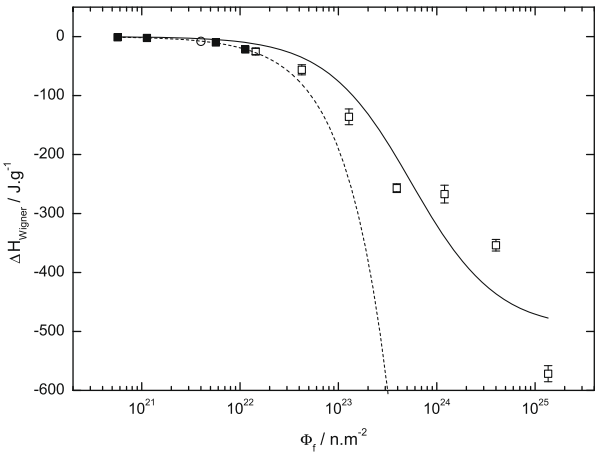

Fig. 2. $\Delta H_{\mathrm{Wigner}}$ released between 25 °C and 375 °C at 10 °C min^{-1} as a function of fast-neutron fluence. ■ – current data, □ – previous data [3], ○ – Iwata [8], solid line – best fit according to Eq. (6), dashed line – linear best fit.

in this fluence range is expected to be linear (Eq. (4)). The linear Wigner energy accumulation rate per unit of fast-neutron fluence, $\alpha_{\Delta H}$, calculated from the current data amounts to $1.90 \pm 0.04 \times 10^{-21}$ J g^{-1} n^{-1} m^2. This compares well with the value of 2×10^{-21} J g^{-1} n^{-1} m^2 derived from Iwata's data [16] but is somewhat lower than our previous value of 7×10^{-21} J g^{-1} n^{-1} m^2 [3]. *The discrepancy can, however, be explained by noting that the fast-neutron fluence values used in [3] were rough estimates subject to a considerable uncertainty and that, at the same fluence, the magnitude of $\Delta H_{\mathrm{Wigner}}$ values measured previously [3] can be no higher than those measured in this work* (see Section 3.2). *Graphically adjusting the fluence associated with the old data to yield a smooth transition to the new data, we have concluded that the fluence values in our previous work [3] were about a factor of 8 too low. Hereafter, unless otherwise stated, all references to our previous work [3] include this correction.* Including the previous $\Delta H_{\mathrm{Wigner}}$ values thus adjusted leads to the situation shown in Fig. 2. The same empirical rational function as before [3], here Eq. (6), was then used to perform a least-squares fit to the combined old and new data. The saturation value is $a = 497 \pm 49$ J g^{-1}, and the value of fluence that leads to a Wigner energy accumulation of one half the saturation value is $b = 5.6 \pm 2.2 \times 10^{23}$ n m^{-2}. Furthermore, $\alpha_{\Delta H} = a/b = 0.9 \pm 0.4 \times 10^{-21}$ J g^{-1} n^{-1} m^2. The fluence at which the Wigner energy accumulation begins to significantly deviate from linearity (e.g., $\Delta H_{\mathrm{Wigner}} \leqslant 0.9\, a/b\, \Phi_f$) is $b/9 \approx 6.2 \times 10^{22}$ n m^{-2}. (The adjusted values of b, $\alpha_{\Delta H}$, and $b/9$ from the old data only would be 5.6×10^{23} n m^{-2}, 0.9×10^{-21} J g^{-1} n^{-1} m^2, and 6×10^{22} n m^{-2}, respectively.) The deviation from linearity thus defined begins at a somewhat higher fluence than the 10^{22} n m^{-2} indicated by Bonjour et al. [13], however, it is seen in Fig. 2 that the data begins to visibly lag behind the calculated linear curve at just about that fluence. Other literature values of $\alpha_{\Delta H}$ are summarized in Table 4. The values of Primak [14] and Platonov et al. [23] are an order of magnitude lower than our 1.9×10^{-21} J g^{-1} n^{-1} m^2 – possibly the result of including data well beyond the linear response region. This effect also manifested itself to some extent in $\alpha_{\Delta H}$ obtained in [3]. The other values [13,16–19] are larger but all within a factor of less than five.

The number of Frenkel defects present in the samples, calculated from Eq. (1) ($\sigma_d = 11.5 \times 10^{-26}$ m^2) and Eq. (2) ($h_F = 14$ eV), is also shown in Table 2. The dpa ratio defined in Eq. (3) is not unity but rather ~6.5 with no discernible effect of fluence. This insensitivity to fluence, combined with the fact that the ratio increases from 7.7 at $\Phi_f = 1.4 \times 10^{22}$ n m^{-2} to 313.7 at $\Phi_f = 1.4 \times 10^{25}$ n m^{-2} [3] is another indication that the current data are representative of the linear response region which extends up to ~10^{22} n m^{-2}. Taking the value of $\alpha_{\Delta H}$ as experimentally well-established, the deviation of the dpa ratio from unity in the linear response region (Eq. (5)) indicates that the product $\sigma_d \cdot h_F$ is too high by a factor of ~6.5. In the absence of independent experimental data on σ_d and/or h_F one can only speculate as to their true values. One such speculation deemed reasonable is to accept $h_F \approx 10.7$ eV as suggested by quantum-mechanical calculations of Telling et al. [20] and Ewels et al. [21] and to conclude that the displacement cross section is somewhat lower than Iwata's value [15] at $\sigma_d \approx 2.3 \times 10^{-26}$ m^2. The value of independent experimental determination of σ_d and/or h_F for a better understanding of the subject can not be overestimated.

4.2. Dimensional changes

A small angular selection of a temperature-resolved X-ray pattern around the 001 diffraction peak of graphite, obtained with a sample irradiated to 1.13×10^{22} n m^{-2} is shown in Fig. 3. A detail between 100 and 300 °C is shown in Fig. 4. No visible changes in the 001 peak position with increasing temperature beyond those

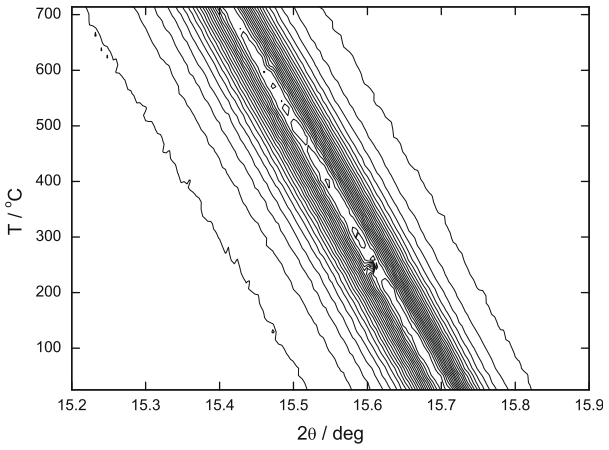

Fig. 3. Temperature-resolved X-ray diffraction pattern, 25–725 °C, in the vicinity of the 002 graphite diffraction peak.

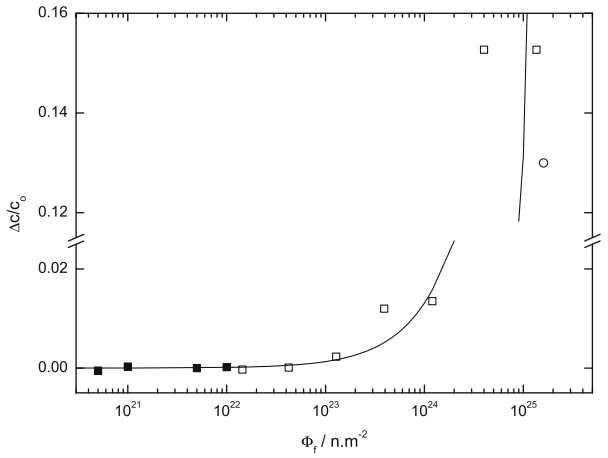

Fig. 5. Relative Lattice Parameter Change $\Delta c/c$ at 25 °C from Rietveld refinement with X-ray diffraction patterns obtained at 25 °C as a function of fast-neutron fluence. ■ – current data, □ – previous data [3], ○ – Kelly et al. [12].

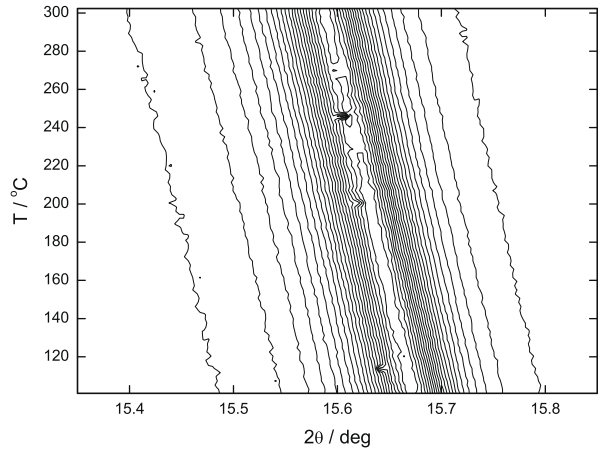

Fig. 4. Detail of a temperature-resolved X-ray diffraction pattern, 100–300 °C, in the vicinity of the 002 graphite diffraction peak.

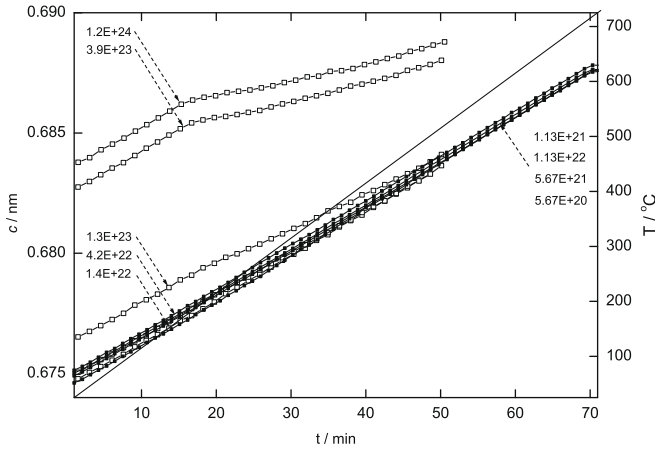

Fig. 6. Graphite c lattice parameter from Rietveld refinement with X-ray diffraction patterns obtained between 25 and 725 °C at 10 °C.min^{-1}. ■ – current data, □ – previous data [3], thin line – temperature. Numbers inside the graph represent fluences in n m^{-2}.

associated with thermal expansion can be seen around 200 °C, where a decrease in slope has previously been observed in more highly irradiated graphite [3]. Results of the Rietveld refinement using two X-ray patterns for each of the four fluence values are shown in Table 2 and Figs. 5 and 6. In Table 2, the value of c at 25 °C is seen to be 0.675 nm, independently of fluence. Using this value, in Fig. 5, the values of $\Delta c/c$ at 25 °C from this and the previous work [3] are plotted. Measurable increase in $\Delta c/c$ from zero begins at a fluence of $\sim 1 \times 10^{23}$ n m^{-2}. Performing a linear least-squares fit on this data according to Eq. (7), excluding the two previous values at 4×10^{20} and 1.36×10^{25} n m^{-2} (obtained from the 001 graphite X-ray diffraction peaks severely widened by high-fluence fast-neutron irradiation), yields $\alpha_{\Delta c}/c = 1.3 \pm 0.2 \times 10^{-26}$ n^{-1} m^2 or $\alpha_{\Delta c} = 0.9 \times 10^{-26}$ nm n^{-1} m^2. This and other available literature values of $\alpha_{\Delta c}$ are summarized in Table 4. There is good agreement with values of Primak [14], Platonov et al. [23], and Kelly et al. [12] which are smaller by a factor of 2–3. And finally, combining the best values of $\alpha_{\Delta H}$ from this work and [3] with $\alpha_{\Delta c}$ from this work, the coefficient $\alpha_{\Delta H}/\alpha_{\Delta c}$ amounts to 1×10^5 J g^{-1} n m^{-1}, compared to 3×10^4 J g^{-1} n m^{-1} [23].

The value of the CTE α_c obtained as an average from all eight DSC/XRD samples as the slope of the (linear) c vs. T curves over the full temperature range (see Fig. 6) is $2.68 \pm 0.1 \times 10^{-5}$ °C^{-1}. This falls comfortably into the literature α_c range of 2.31–2.83×10^{-5} °C^{-1} and is thus proposed here as the best value of α_c. Because of the low fluences involved, no effect on α_c^{25} could be ascertained. Although indications of an increase of α_c with temperature, in accordance with literature data, have been observed, its reasonable quantification has not been possible. The value of the CTE α_a obtained as an average from all eight DSC/XRD samples as the slope of the (linear) a vs. T curves over the full temperature range (not shown in Fig. 6) is $-3 \pm 3 \times 10^{-6}$ °C^{-1}. The error of the current value is such that the whole range of the literature α_a values of -1.0 to -1.5×10^{-6} °C^{-1} is encompassed. Additionally, the literature values are likely to be associated with significant errors as well so that $\alpha_a = -2 \times 10^{-6}$ °C^{-1} is proposed here as a reasonable estimate. No effects of fluence on α_a[25] and/or temperature on α_a could be determined.

5. Conclusion

Graphite irradiated at a TRIGA Mark II research reactor to a fast-neutron fluence from 5.67×10^{20} to 1.13×10^{22} n m^{-2} at a fast-neutron flux ($E > 0.1$ MeV) of 7.88×10^{16} n m^{-2} s^{-1} and at temperatures not exceeding 100 °C, exhibits Wigner energies ranging from 1.2 to 21.8 J g^{-1}. The Wigner energy accumulation rate is $\alpha_{\Delta H} = 1.9 \times 10^{-21}$ J g^{-1} n^{-1} m^2. The DSC curves exhibit, in addition

to the well known peak at ~200 °C, a pronounced fine structure consisting of additional peaks at ~150 °C, ~230 °C, and ~280 °C. These peaks correspond to activation energies of 1.31 eV, 1.47 eV, 1.57 eV, and 1.72 eV, respectively. Crystal structure of the samples is intact. The c lattice parameter increase rate is $\alpha_{\Delta c} = 0.9 \times 10^{-26}$ nm n^{-1} m^2. The dependence of the c lattice parameter on temperature between 25 °C and 725 °C as determined by Rietveld refinement leads to the expected microscopic thermal expansion coefficient along the c axis of $\sim 26 \times 10^{-6}$ °C^{-1}. At 200 °C, coinciding with the maximum in the differential-scanning-calorimeter curves, no measurable changes in the rate of thermal expansion have been detected – unlike its decrease previously seen in more highly irradiated graphite. A useful correlation factor between Wigner energy accumulation, ΔH_{Wigner}, and the c lattice parameter increase, Δc, amounts to $\alpha_{\Delta H}/\alpha_{\Delta c} = 1 \times 10^5$ J g^{-1} n m^{-1}, allowing an estimation of ΔH_{Wigner} from experimentally determined Δc and vice versa. An independent experimental determination of the displacement cross section, σ_d, and/or Frenkel defect energy, h_F, would greatly contribute to a better understanding of the subject on a microscopic level.

Acknowledgements

The samples were machined with great skill by H. Baumgartner. Some of the XRD data preparation and evaluation was performed by Ms. E. Ruppert during her summer internship with the first author.

Funding for the purchase of the The PerkinElmer Diamond DSC and DSC 7 instruments has been provided by the Austrian Federal Ministry of Agriculture, Forestry, Environment, and Water Management under Contract No. BMLFUW-Zl. 57 4308/6-V/7/03.

This research project has been supported by the European Commission under the 6th Framework Program through the Key Action: Strengthening the European Research Area, Research Infrastructures, Contract No. RII3-CT-2004-506008.

References

[1] E.P. Wigner, CP-387, 1942, p. 4.
[2] E.P. Wigner, J. Appl. Phys. 17 (1946) 857.
[3] D. Lexa, A.J. Kropf, J. Nucl. Mater. 348 (2006) 122.
[4] H.W. Weber, H. Böck, E. Unfried, L.R. Greenwood, J. Nucl. Mater. 137 (1986) 236.
[5] B.D. Patterson et al., Nucl. Instr. and Meth. A 540 (2005) 42.
[6] D. Lexa, Thermochim. Acta 398 (2003) 241.
[7] B. Schmitt et al., Nucl. Instr. and Meth. A 501 (2003) 267.
[8] A.C. Larson, R.B. Von Dreele, Los Alamos National Laboratory Report LAUR 86-748, 1994.
[9] T.J. Neubert, M. Burton, R.C. Hirt, A.R. VanDyken, M.G. Bowman, J. Royal, W.R. Burns, A. Novick, R. Maurer, R. Ruder, Argonne National Laboratory Report ANL-5472, 1956.
[10] F. Seitz, Dics. Faraday Soc. 5 (1949) 271.
[11] P.A. Thrower, R.M. Mayer, Phys. Stat. Sol. 47 (1978) 11.
[12] B.T. Kelly, B.J. Marsden, K. Hall, D.G. Martin, A. Harper, A. Blanchard, IAEA-TECDOC-1154, 2000.
[13] E. Bonjour, J. Doulat, P. Mas, P.R. Goggin, Radiation Damage in Reactor Materials, IAEA, Vienna, 1969. p. 83.
[14] W. Primak, Phys. Rev. 103 (1956) 1681.
[15] T. Iwata, S. Takamura, H. Maeta, T. Aruga, IAEA-TECDOC-263, 1982, p. 175.
[16] T. Iwata, J. Nucl. Mater. 133&134 (1985) 361.
[17] E.W.J. Mitchell, M.R. Taylor, Nature 208 (1965) 638.
[18] L. Bochirol, E. Bonjour, Carbon 6 (1968) 661.
[19] L. Bochirol, E. Bonjour, E. Weil, Radiation Damage in Reactor Materials, IAEA, Vienna, 1963. p. 509.
[20] R.H. Telling, C.P. Ewels, A.A. El-Barbary, M.I. Heggie, Nature Mater. 2 (2003) 333.
[21] C.P. Ewels, R.H. Telling, A.A. El-Barbary, M.I. Heggie, P.R. Briddon, Phys. Rev. Lett. 91 (2003) 025505.
[22] P.C. Minshall, A.J. Wickham, in: Proceedings of the Technical Committee Meeting 'Nuclear Graphite Waste Management', IAEA, Manchester, 1999.
[23] P.A. Platonov, E.V. Burlakov, O.K. Chugunov, A.I. Dostov, V.M. Alekseev, E.I. Smorodkin, Atom. Energ. 94 (2003) 225.
[24] Y.S. Touloukian et al. (Eds.), Thermophysical Properties of Matter, vols. 12&13, IFI Plenum, New York, 1971.
[25] A.G. Khodolenko, K. Heinzinger, H.-G. Moser, IHEP Preprint 2001-32, Protvino, 2001, p. 9.